REGIONAL PHOTOMETRY OF ASTEROID RYUGU WITH MULTIPLE PHOTOMETRIC MODELS. Y. Yokota[1], R. Honda[2], D. Domingue[3], E. Tatsumi[4], S. E. Schröder[5], M. Matsuoka[6], L. Riu[7], A. Longobardo[8], S. Sugita[9], T. Morota[9], N. Sakatani[10], C. Honda[11], Y. Cho[9], S. Kameda[10], T. Kouyama[12], M. Yamada[13], M. Hayakawa[1], H. Senshu[13], H. Suzuki[14], K. Yoshioka[9], H. Sawada[1], and K. Ogawa[1], [1]ISAS/JAXA, (3-1-1 Yoshino-dai, Chuo-ku, Sagamihara, Kanagawa, Japan, yokota@planeta.sci.isas.jaxa.jp). [2]Kochi Univ., Japan, [3]Planetary Science Institute, USA, [4]Instituto de Astrofisica de Canarias, Univ. of La Laguna, Spain, [5]DLR, Germany, [6]Observatoire de Paris, France, [7]Univ. Paris-Saclay, France, [8]INAF, Italy, [9]Univ. of Tokyo, Japan, [10]Rikkyo Univ., Japan. [11]Univ. of Aizu, Japan. [12]AIST, Japan, [13]Chiba Inst. Tech, Japan, [14]Meiji Univ., Japan.

Introduction: The surface of the Cb-type asteroid Ryugu (equatorial radius = 502 ±2 m [1]) is divided into the Western bulge and Eastern hemisphere by troughs [1,2,3] (Figure 1). The Western bulge has fewer craters [4] and fewer boulders (D>5 m) [5] than the Eastern hemisphere. Previous photometric studies [2,6] in visible wavelengths using the Hayabusa2 Telescopic Onboard Navigation Camera (ONC-T) images reported that the western bulge has a slightly higher v-band (0.55 μm) reflectance than that of the Eastern hemisphere. A similar dichotomy is also seen in Near-Infrared [7]. However, opposition (zero phase angle) observations revealed that both regions showed similar normal albedo [8]. We hypothesized that the east-west difference might be a result of surface structural properties (such as roughness) rather than albedo, therefore we performed regional photometric analyses. In our previous study [9], we modeled photometric data extracted from the imaging data set and derived two Hapke parameters for low latitude region. To verify the results, we extended the analysis to use a Hapke model [10,11] with three free parameters and applied other empirical photometric models, the Kaasalainen-Shkuratov set of models [12,13].

Data and methods: We divided the Ryugu surface into meshes of ~32 meters square and created a database of the intensity of the reflected light (radiance factor, I/F) and the angles of observation (*i*,*e*,*α*) for seven sets of observations on each mesh. Details are described in [9].

Hapke model. The Hapke model we use has five parameters: the single scattering albedo (*w*), the scattering function parameter amplitude (*b*), the opposition surge width (*h*) and strength (B_0), and the macroscopic roughness (θ-bar). Since it is difficult to separate all five parameters from the limited phase angle range (0 to 40 degrees) of this data set, we first performed the fitting varying only two parameters (*w* and θ-bar), using the Levenberg-Marquardt method. Other parameters were fixed by the values of [6]. We then re-modeled the data using three free parameters (*w*, *h*, and θ-bar).

Kaasalainen-Shkuratov set of models. The I/F of the data set was fitted using the equation

$$I/F = A_n e^{-\alpha v} * D(i,e), \quad (1)$$

where A_n is the normal albedo, $e^{-\alpha v}$ is the phase function, and $D(i,e)$ is one of the five disk functions: 1) the Lommel-Seeliger, D_{ls}, disk function, 2) the Lommel-Seeliger-Lambert, D_{lsl}, function, 3) the Minnaert, D_m, function, 4) the Akimov, D_a, disk function, and 5) the Akimov-Shkuratov, D_{as}, disk function. These are given by

$$D_{ls} = \frac{2cosi}{cosi+cose}, \quad (2)$$

$$D_{LSL} = c_l\left(\frac{2cosi}{cosi+cose}\right) + (1-c_l)cosi, \quad (3)$$

$$D_M = cosi^k cose^{k-1}, \quad (4)$$

$$D_a = cos\left(\frac{\alpha}{2}\right) cos\left[\frac{\pi}{\pi-\alpha}\left(\gamma-\frac{\alpha}{2}\right)\right]\frac{(cos\beta)^{\alpha/(\pi-\alpha)}}{cos\gamma}, \quad (5)$$

$$D_{as} = cos\left(\frac{\alpha}{2}\right) cos\left[\frac{\pi}{\pi-\alpha}\left(\gamma-\frac{\alpha}{2}\right)\right]\frac{(cos\beta)^{\eta\alpha/(\pi-\alpha)}}{cos\gamma}, \quad (6)$$

where the D_{ls} and D_a disk functions have no free parameters and the D_{lsl}, D_m, and D_{as} disk functions have a single free parameter (c_l, k, η, respectively) each. These models have been applied to image data of the Moon [13], Vesta [14], and Mercury [15].

The free parameters include *An*, *ν*, and if relevant, a disk function parameter. The equations were fit in an iterative method using a least squares grid search [6].

Since we are still in the middle of the trial run, we have applied the grid search only to those areas (28% of the total surface) where the variation of incidence and emission angles is large.

Results: Figure 2 shows the parameter maps of the Ryugu surface obtained from the Hapke model in the 2 free parameter case. The distribution of *w* was similar to the normal albedo distribution [8], and there was little difference between east and west. The roughness parameter, θ-bar, showed a difference between east and west. Since only two parameters are used here, another approach is needed to understand if the differences in θ-bar are attributable only to roughness.

Figure 3 shows the parameter maps for the Hapke model in the 3 free parameter case. Here, *w* is almost the same as in Figure 2a. This provides confidence that the single scattering albedo is reasonable determined. On the other hand, Figure 3b and 3c show that the

distribution in Figure 2b has been distributed between two parameters. The difference between east and west is weaker in terms of roughness. Whether figure 3b is more reliable than Figure 2b as a result of roughness needs to be further examined.

For the Kaasalainen-Shkuratov set of models, parameter estimates have been identified for the first time for Ryugu surfaces (Table 1). The application to the whole globe is still to be done, however, the normal albedo values (median ~0.041) are consistent with previous studies [6,8]. Once we have the global parameter distribution, we will see if the disk function parameter correlates with Figure 2b, 3b, or 3c.

Acknowledgments: This study was supported by JSPS Core-to-Core program International Network of Planetary Sciences. D.D. was supported by NASA's Hayabusa2 Participating Scientist (NNX16AL34G) and SSERVI/TREX (NNH16ZDA001N) programs.

References: [1] Watanabe S. et al. (2019) *Science 364*, 268. [2] Sugita S. et al. (2019) *Science 364*, 252. [3] Hirabayashi M. et al. (2019) *ApJL 874*, L10. [4] Cho Y. et al. (2021) *JGR 126*, e2020JE006572. [5] Michikami T. et al. (2019) *Icarus* 331, 179–191. [6] Tatsumi E. et al. (2020) *A&A 639*, A83. [7] Barucci M.A. et al. (2019) *A&A 629*, A13. [8] Yokota Y. et al. (2021) *Planet. Sci. J. 2*, 177. [9] Yokota Y. et al. (2021) *LPS 52nd*, Abstract #2105. [10] Hapke B. (1981) *JGR* 86(B4), 3039–3054. [11] Hapke B. (2012) Theory of Reflectance and Emittance Spectroscopy (2nd ed.). Cambridge Univ. Press. [12] Kaasalainen M. et al. (2001) *Icarus 153*, 37-51. [13] Shkuratov Y. et al. (2011) *PSS 59*, 1326-1371. [14] Schröder S. et al. (2014) *PSS* 103, 66-81. [15] Domingue D. et al. (2016) *Icarus* 268, 172-203. Tatsumi E. et al. (2020).

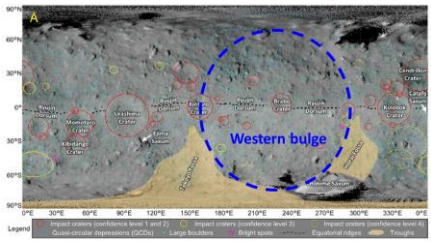

Figure 1. Geology of Ryugu surface (after [2]). The western bulge region is roughly indicated by a blue dashed circle. Pale orange regions are troughs.

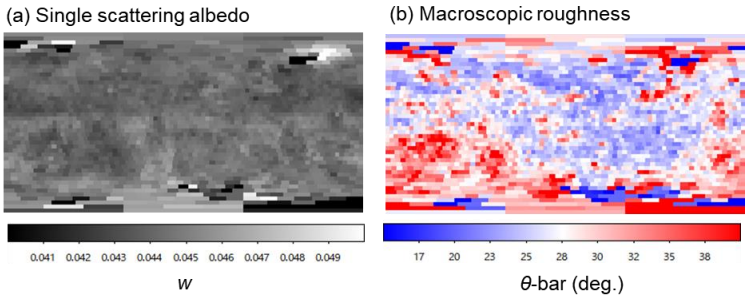

Figure 2. Maps of the derived Hapke parameters (2 free parameter case)

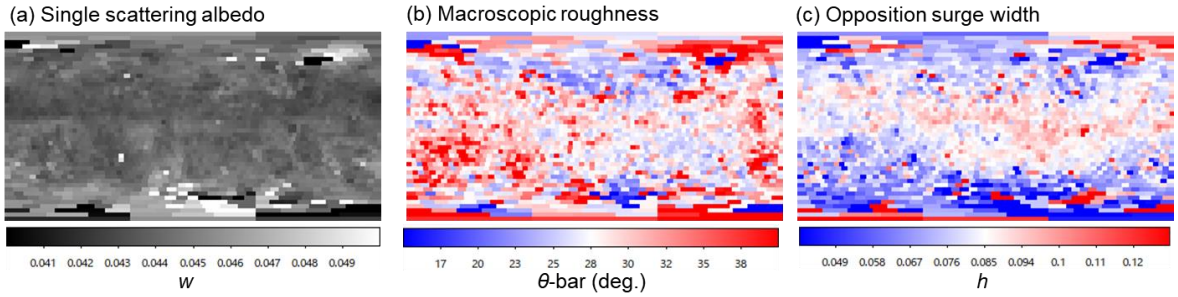

Figure 3. Maps of the derived Hapke parameters (3 free parameter case)

Table 1. Kaasalainen-Shkuratov Set of Models Results: Range of Parameter Values‡

Parameter	Lommel-Seeliger	Lommel-Seeliger-Lambert	Minneart	Akimov	Akimov-Shkuratov
A_n					
Minimum	0.039 ± 0.051	0.039 ± 0.002	0.039 ± 0.002	0.039 ± 0.051	0.039 ± 0.002
Maximum	0.045 ± 0.051	0.045 ± 0.002	0.045 ± 0.002	0.045 ± 0.051	0.045 ± 0.002
Median	0.041 ± 0.051	0.041 ± 0.002	0.041 ± 0.002	0.041 ± 0.051	0.041 ± 0.002
ν					
Step 3 median value	2.6	1.95	1.85	2.3	2.25
Disk Parameter					
Minimum	N/A	0.80 ± 0.05	0.470 ± 0.05	N/A	0 ± 1.045
Maximum	N/A	1.08 ± 0.05	0.585 ± 0.05	N/A	3.995 ± 1.045
Median	N/A	0.93 ± 0.05	0.525 ± 0.05	N/A	3.995 ± 1.045

‡ Error listed is the median error across all data sets.